Plant Physiology, September 1999, Vol. 121, pp. 97–111, www.plantphysiol.org © 1999 American Society of Plant Physiologists

Stress-Induced Legume Root Nodule Senescence. Physiological, Biochemical, and Structural Alterations[1]

Manuel A. Matamoros, Lisa M. Baird, Pedro R. Escuredo, David A. Dalton, Frank R. Minchin, Iñaki Iturbe-Ormaetxe, Maria C. Rubio, Jose F. Moran, Anthony J. Gordon, and Manuel Becana*

Departamento de Nutrición Vegetal, Estación Experimental de Aula Dei, Consejo Superior de Investigaciones Científicas, Apdo 202, 50080 Zaragoza, Spain (M.A.M., P.R.E., I.I.-O., M.C.R., J.F.M., M.B.); Biology Department, University of San Diego, San Diego, California 92110 (L.M.B.); Biology Department, Reed College, Portland, Oregon 97202 (D.A.D.); and Institute of Grassland and Environmental Research, Plas Gogerddan, Aberystwyth SY23 3EB, United Kingdom (F.R.M., A.J.G.)

Nitrate-fed and dark-stressed bean (*Phaseolus vulgaris*) and pea (*Pisum sativum*) plants were used to study nodule senescence. In bean, 1 d of nitrate treatment caused a partially reversible decline in nitrogenase activity and an increase in O_2 diffusion resistance, but minimal changes in carbon metabolites, antioxidants, and other biochemical parameters, indicating that the initial decrease in nitrogenase activity was due to O_2 limitation. In pea, 1 d of dark treatment led to a 96% decline in nitrogenase activity and sucrose, indicating sugar deprivation as the primary cause of activity loss. In later stages of senescence (4 d of nitrate or 2–4 d of dark treatment), nodules showed accumulation of oxidized proteins and general ultrastructural deterioration. The major thiol tripeptides of untreated nodules were homoglutathione (72%) in bean and glutathione (89%) in pea. These predominant thiols declined by approximately 93% after 4 d of nitrate or dark treatment, but the loss of thiol content can be only ascribed in part to limited synthesis by γ-glutamylcysteinyl, homoglutathione, and glutathione synthetases. Ascorbate peroxidase was immunolocalized primarily in the infected and parenchyma (inner cortex) nodule cells, with large decreases in senescent tissue. Ferritin was almost undetectable in untreated bean nodules, but accumulated in the plastids and amyloplasts of uninfected interstitial and parenchyma cells following 2 or 4 d of nitrate treatment, probably as a response to oxidative stress.

Legume N_2 fixation is particularly sensitive to environmental perturbations, including defoliation, water deficit, continuous darkness, and nitrate fertilization (Vance et al., 1979; Witty et al., 1986; Layzell et al., 1990). In most types of stress, the initial decrease of nitrogenase activity is associated with a decline in the O_2 concentration reaching the infected cells and bacteroids (Witty et al., 1986; Carroll et al., 1987; Layzell et al., 1990; Escuredo et al., 1996). Prolongation of stress induces premature nodule senescence, which shares some features with natural senescence (nodule aging), such as the loss of N_2 fixation, the increase in lytic activities, and the formation of green pigments from leghemoglobin (Lb) (Pfeiffer et al., 1983; Sarath et al., 1986). This stress-induced senescence has been linked to the enhanced production of oxidants and the lowering of antioxidant defenses (Escuredo et al., 1996; Gogorcena et al., 1997). Oxidants include inorganic (H_2O_2) and organic (lipid) peroxides as well as "catalytic iron," the fraction of iron in plant tissues capable of catalyzing the generation of hydroxyl radicals through Fenton reactions (Becana et al., 1998).

A major antioxidant mechanism operating in the nodule cytosol is the ascorbate-GSH cycle, which results ultimately in the detoxification of H_2O_2 at the expense of NAD(P)H. The pathway involves the concerted action of four enzymes: ascorbate peroxidase (APX), dehydroascorbate reductase (DR), monodehydroascorbate reductase (MR), and glutathione reductase (GR), and requires a continuous supply of ascorbate, thiols, and reduced pyridine nucleotides (Dalton et al., 1986, 1992). The initial enzyme of the pathway, APX, may account for up to 1% of the total soluble protein of nodules (Dalton et al., 1998). The thiol tripeptide GSH (γGlu-Cys-Gly) also participates in the removal of peroxides through the ascorbate-GSH cycle, but it performs additional roles in plants, such as the transport and storage of sulfur, the control of redox status, and the detoxification of heavy metals (Rennenberg, 1995; May et al., 1998). The synthesis of GSH involves two ATP-dependent reactions catalyzed by the enzymes γ-glutamylcysteinyl synthetase (γECS) and GSH synthetase (GSHS). Thiol tripeptides are particularly abundant in the leaves, roots, and seeds of legumes, where a thiol tripeptide homolog homoglutathione (hGSH; γGlu-Cys-βAla), may be present in addition to or instead of GSH (Klapheck, 1988). Apparently, a specific hGSH synthetase (hGSHS) catalyzes the second step of hGSH synthesis in the leaves of some legumes (Macnicol, 1987; Klapheck et al., 1988). It is not known whether hGSH and hGSHS are present in the nodules.

An entirely different antioxidant mechanism involving the sequestration of catalytic iron by ferritin may also operate in the nodules. Plant ferritins are composed of 24 subunits and can store up to 4,500 atoms of iron in a safe,

[1] This work was supported by grant nos. PB95–0091 and PB98–0522 from the Dirección General de Enseñanza Superior e Investigación Científica (Ministry of Education and Culture, Spain) to M.B., and by fellowships from the Gobierno Vasco (M.A.M.), the European Union (I.I.-O.), and the Ministry of Education and Culture (P.R.E., M.C.R., J.F.M.).

* Corresponding author; e-mail becana@eead.csic.es; fax 34–976–575620.

nontoxic form (Briat and Lobréaux, 1997). In nodules, ferritin may also act as an iron reservoir for nitrogenase, Lb, and other iron-proteins, since ferritin protein increases early in nodulation and then declines concomitantly with the increase in nitrogenase activity, heme, and non-heme iron (Ragland and Theil, 1993). However, little is known about ferritin in senescent nodules. This information may be of considerable interest because nodules are extremely rich in iron (Ragland and Theil, 1993) and this may become available (catalytic iron) for Fenton reactions by proteolysis during nodule senescence, either natural or induced by stress (Becana et al., 1998).

Many other important alterations related to oxygen, carbon, and nitrogen metabolism occur in nodules during senescence, but the precise sequence of these biochemical changes is far from clear (Carroll et al., 1987; Layzell et al., 1990; Gordon et al., 1997). There is also a paucity of information regarding the structural changes involved in stress-induced nodule senescence. Light and electron microscopy studies have been carried out with nodules of detopped alfalfa (Vance et al., 1979), dark-treated soybean (Cohen et al., 1986), and nitrate-treated lupine (Lorenzo et al., 1990). Nevertheless, legume symbioses differ in their tolerance to stress, and at least some of these differences may be related to the growth pattern (indeterminate versus determinate) of nodules (Sprent, 1980). Comparison of the inhibitory effects of stress on other legumes may provide insight into the mechanisms underlying stress tolerance and nodule senescence.

The general objective of the present study was to ascertain the time course of events leading to the loss of function and structural deterioration of nodules following stress application to the plant. The specific objective was to gain further information on the role of some important antioxidants (APX, thiols, and ferritin) in the protection of legume N_2 fixation against the noxious effects of peroxides, free radicals, and catalytic iron. Data presented in this paper are intended to complement two previous reports (Escuredo et al., 1996; Gogorcena et al., 1997) in providing an orthogonal comparison of nitrate- and dark-stress-induced senescence in determinate and indeterminate nodules.

MATERIALS AND METHODS

Plants and Treatments

Nodulated bean (*Phaseolus vulgaris* L. cv Contender × *Rhizobium leguminosarum* bv *phaseoli* 3622) and pea (*Pisum sativum* L. cv Lincoln × *R. leguminosarum* bv *viciae* NLV8) plants were grown in a perlite:vermiculite mixture (2:1) in controlled-environment chambers as described by Gogorcena et al. (1997). When bean had reached the late-vegetative stage (30–32 d), pots were divided at random into three groups receiving 10 mM potassium nitrate for 1, 2, or 4 d, and one group of controls receiving N-free nutrient solution and harvested on the 3rd d. Likewise, when pea plants had reached the late-vegetative stage (34–36 d), pots were divided at random into three groups placed in the dark (with otherwise identical conditions) for 1, 2, or 4 d, and one group of controls kept in the light and harvested on the 3rd d. These control plant harvests were arranged so that the maximum age difference between treated and control plants was 2 d. The same protocol was used to produce dark-treated bean and nitrate-treated pea plants so as to obtain nodules for microscopic studies. Nodules to be used for light and electron microscopic analyses were fixed immediately upon detachment, as described under "Light Microscopy Studies." Nodules to be used for biochemical analyses were flash-frozen in liquid N_2 and stored at −80°C for later analysis (within 4–5 weeks).

Nodule Activity and Carbon Metabolites

Nitrogenase activity and root respiration of intact, undisturbed plants were measured simultaneously using a flow-through gas system (Minchin et al., 1983) housed in a controlled-environment chamber. Root systems were sealed in the growth pots and allowed to stabilize for 18 h. In vivo nitrogenase activity was measured as H_2 evolution (Witty and Minchin, 1998) using electrochemical H_2 sensors (City Technology, Portsmouth, UK) and respiratory CO_2 production was measured using an IR gas analyzer. Measurements were made in air for 5 min and then in a gas stream of 79% (v/v) Ar/21% (v/v) O_2. Following exposure to Ar/O_2, steady-state conditions were reached after 60 to 80 min and the external O_2 concentration was then increased over the range of 21% to 60% (8.55–24.54 mmol O_2 L^{-1}) in steps of 5% or 10%. Each increase in O_2 took 5 to 6 min and was followed by a 20- to 25-min equilibration period. These data were used to calculate the oxygen diffusion barrier (ODB) resistance and carbon costs of nitrogenase, as described in Escuredo et al. (1996).

Based on the maximum H_2 production under Ar/O_2, the electron allocation coefficient for N_2 was 0.67 for control pea nodules and 0.73 for control bean nodules. The *hup*-negative genotype of the two *Rhizobium* strains used in these studies was confirmed by Southern-blot analysis of *Eco*RI-digested total DNA using a *hup*-specific DNA probe prepared by dioxigenin labeling of cosmid pAL618 containing the entire *hup* gene cluster from *Rhizobium leguminosarum* bv *viciae* strain UPM791 (Leyva et al., 1990).

Lb was determined by a method based on the fluorescence emitted by the tetrapyrrol ring after removal of iron by hot, saturated oxalic acid (LaRue and Child, 1979) using myoglobin (horse skeletal muscle, Calbiochem) as the standard. Protein of the nodule cytosol and bacteroids was determined with a commercial dye (Bio-Rad) using crystalline BSA (Sigma) as the standard. Total lipids were extracted from nodules at room temperature essentially as described by Bligh and Dyer (1959).

Carbohydrates were extracted from 0.2 g of nodules with 10 mL of boiling 80% (v/v) ethanol. The ethanol-soluble extracts were dried in vacuo at 40°C and the soluble compounds redissolved in 4 mL of water. The samples were centrifuged at 20,000*g* for 10 min, and the contents of Glc, Fru, and Suc were determined spectrophotometrically at 340 nm using enzymatic assays coupled to the formation of NADH (González et al., 1995). Starch was extracted from the ethanol-insoluble residue and quantified as the Glc

released following digestion with amyloglucosidase (MacRae, 1971).

Catalase and Enzymes of the Ascorbate-GSH Cycle

Antioxidant enzymes were extracted at 4°C from 0.5 g (bean) or 0.25 g (pea) of nodules with a mortar and pestle. Catalase and APX were extracted with 10 mL (bean) or 5 mL (pea) of 50 mM potassium phosphate buffer (pH 7.0) containing 0.5% (w/v) PVP-10. DR, GR, and MR were extracted with 5 mL (bean) or 2.5 mL (pea) of 50 mM potassium phosphate buffer (pH 7.8) containing 1% (w/v) PVP-10, 0.2 mM Na_2EDTA, and 10 mM β-mercaptoethanol. The homogenate was filtered through one layer of Miracloth (Calbiochem) and centrifuged at 15,000*g* for 20 min.

Catalase activity was assayed by following the decomposition of H_2O_2 at 240 nm (Aebi, 1984). APX and DR activities were determined by measuring the oxidation of ascorbate at 290 nm (Asada, 1984) and the formation of ascorbate at 265 nm (Nakano and Asada, 1981), respectively. MR and GR activities were assayed by monitoring the oxidation of NADH (Dalton et al., 1992) and NADPH (Dalton et al., 1986) at 340 nm, respectively.

All activities were measured at 25°C in 1-mL reaction mixtures within the linear range. Measurements were made with a spectrophotometer (Lambda-16, Perkin-Cetus) during the first 1.5 to 3 min with no lag period (except for APX, which was measured after a lag of 40 s). Assays were made using sample volumes ranging from 10 (catalase) to 100 μL (GR). Where appropriate, controls made by omitting or boiling extracts were run in parallel to correct for nonenzymatic rates, and buffers and reagents were treated with Chelex resin to avoid contamination by trace amounts of transition metal ions.

Thiols and Thiol Synthetase Activities

GSH and hGSH were extracted from 50 mg of nodules with 500 μL of 200 mM methanesulfonic acid containing 0.5 mM diethylenetriaminepentaacetic acid. After centrifugation at 13,000*g* for 5 min, the supernatant was derivatized at pH 8.0 with 2 mM monobromobimane (Fahey and Newton, 1987). The bimane derivatives of GSH and hGSH were separated and quantified by HPLC (Waters) using an analytical C_{18} column (3.9 × 150 mm; 4 μm; Nova-Pak, Waters) and a 15% (v/v) methanol/0.25% (v/v) acetic acid (pH 3.5) solvent at a constant flow of 1 mL min^{-1}. Detection was by fluorescence (model 474 scanning fluorescence detector, Waters) with excitation at 380 nm and emission at 480 nm. Standards of GSH (Sigma) and hGSH (obtained by chemical synthesis at the University of Nebraska, Lincoln) were processed identically to the samples. The proportion of thiol tripeptides present in the oxidized form was determined by an enzymatic recycling procedure using yeast GR to reduce the disulfide forms and vinylpyridine as a thiol blocking agent (Griffith, 1980; Law et al., 1983).

The extraction and assays of γECS, GSHS, and hGSHS activities were performed by modification of previous protocols, based on the HPLC separation of synthesized γGluCys, GSH, and hGSH after derivatization with monobromobimane (Hell and Bergmann, 1988; Kocsy et al., 1996).

Other Metabolites

Ascorbate was extracted from 0.25 g of nodules with 5 mL of 5% (w/v) metaphosphoric acid and quantified by a method based on the ascorbate-dependent reduction of iron (III) to iron (II). Formation of the complex between iron (II) with 2,2′-dipyridyl was measured at 525 nm (Law et al., 1983).

Pyridine nucleotides were extracted from 30 mg of nodules with 2× 0.5 mL of 0.1 M NaOH (NADH and NADPH) or with 2× 0.5 mL of 5% (w/v) TCA (NAD^+ and $NADP^+$) at room temperature. After thorough homogenization for 90 to 120 s in an Eppendorf tube, the extracts were boiled for 6 min, cooled on ice, and centrifuged at 13,000*g* for 6 min at room temperature. The supernatant (25 μL for bean and 50 μL for pea) was made up to 100 μL with NaOH or TCA, and the nucleotides were quantified by the enzymatic cycling method of Matsumura and Miyachi (1980).

Oxidant Damage

Lipid peroxides were extracted from 0.5 g of nodules with 5 mL of 5% (w/v) metaphosphoric acid and 100 μL of 2% (w/v in ethanol) butyl hydroxytoluene (Minotti and Aust, 1987). The extract was filtered through one layer of Miracloth and centrifuged at 15,000*g* for 20 min. An aliquot of the supernatant was reacted with thiobarbituric acid at low pH and 95°C and cooled to room temperature. The resulting thiobarbituric acid-malondialdehyde adduct was extracted with 1-butanol and quantified by HPLC as described in detail by Iturbe-Ormaetxe et al. (1998).

Protein carbonyl content was measured by derivatization with 2,4-dinitrophenyl-hydrazine as indicated by Levine et al. (1990) with some modifications. Proteins were extracted from 0.5 g of nodules with 5 mL of 100 mM potassium phosphate (pH 7.0), 0.1% (v/v) Triton X-100, 1 mM Na_2EDTA, and 2.5 μg each of aprotinin and leupeptin to prevent proteolysis of oxidized proteins during sample preparation. After precipitation of possible contaminating nucleic acids in the samples with 1% (w/v) streptomycin sulfate, an aliquot of 0.8 mL of the extracts was reacted with 0.2 mL of 20 mM dinitrophenylhydrazine (in 2 M HCl), and another aliquot (control) with 0.2 mL of 2 M HCl for 1 h, with vigorous shaking every 10 to 15 min. Proteins were then precipitated with 10% (w/v) TCA, and the pellet was washed four times with 1:1 (v/v) ethanol:ethyl acetate. Precipitated proteins were solubilized in 6 M guanidine-HCl (pH 4.5) by incubation for 30 min with shaking. The insoluble material was removed by centrifugation, and the absorbance of the hydrazones (derivatized carbonyls) was measured at 370 nm (Levine et al., 1990). To obtain more accurate results, the amount of protein to be analyzed for carbonyl content was adjusted to 0.5 mg in all samples.

Light Microscopy Studies

Prior to immunodetection of relevant proteins at the light or electron microscope levels, bean and pea nodule

extracts were subjected to western analysis (Cresswell et al., 1992). Polyclonal antibodies used in this study were raised in rabbits against nitrogenase (universal antibody to the ferroprotein of nitrogenase; courtesy of Dr. Paul Ludden, University of Wisconsin, Madison), APX (soybean nodule cytosol; Dalton et al., 1993, 1998), and ferritin (soybean seeds; courtesy of Dr. Elizabeth Theil, Children's Hospital Oakland Research Institute, Oakland, CA).

Nodules to be used for immunodetection of nitrogenase and APX were fixed overnight in 2% (v/v) paraformaldehyde, 1.25% (v/v) glutaraldehyde, and 50 mM PIPES (pH 7.2). Fixed samples were dehydrated in an ethanol series, embedded in LR White resin, and cut into 1-μm sections with a microtome (Reichert Ultracut R, Leica, Deerfield, IL). For light microscopy immunogold staining, slides were incubated overnight at room temperature in a 1:50 dilution of antibodies raised against nitrogenase or APX. For both antigens, the slides were incubated for 1 h with secondary antibody consisting of affinity-purified goat anti-rabbit IgG conjugated to colloidal gold (Auroprobe, Amersham) at a 1:40 dilution. Silver enhancement solution (InsenSEM, Amersham) was applied at room temperature and monitored for sufficient development (15–25 min) following the protocols of the manufacturer. All sections were counterstained with 0.5% (w/v) safranin in water for 60 s. Representative nodule sections were photographed with a microscope (Laborlux S, Leica) equipped with a camera (FE-2, Nikon).

For light microscopy immunofluorescence staining of APX, the secondary antibody consisted of affinity-purified goat anti-rabbit antibodies conjugated to a Cy3 fluorophore (excitation at 550 nm and emission at 570 nm; Jackson ImmunoResearch Laboratories, West Grove, PA) at a dilution of 1:300 for 30 min. Sections were viewed with the light microscope equipped with a rhodamine filter.

Electron Microscopy Studies

Ultrastructural studies and immunolocalization of APX and ferritin at the electron microscopy level were carried out as indicated in Dalton et al. (1993), except that the APX and ferritin antibodies were used at dilutions of 1:500 and 1:25, respectively, and grids were counterstained only with uranyl acetate. Nodule sections were obtained with a Reichert Ultracut E microtome, and representative micrographs for all treatments were taken with a transmission electron microscope (model 900T, Zeiss) at 80 kV.

RESULTS

Nitrogenase Activity and Related Parameters

Bean plants were treated with 10 mM nitrate for up to 4 d to progressively induce nodule senescence, which was monitored by measuring general markers of metabolic activity (Table I). One day of nitrate application was sufficient to inhibit the in vivo nitrogenase activity by 73% and to increase the ODB resistance by 3-fold. At this stage, the total root respiration and carbon cost of nitrogenase did not vary, but there were significant increases in Lb and total soluble protein of nodules (Table I). After 2 d with nitrate, the carbon cost of nitrogenase increased 1.7-fold, whereas Lb and soluble protein returned to control values. After 4 d there was a further increase in the carbon cost of nitrogenase up to 2.4-fold and decreases of 53% and 31% in Lb and soluble protein, respectively, relative to the control. An increase in rhizosphere O_2 produced a recovery of nitrogenase activity at all stages of the nitrate treatment. Maximum activities at increased O_2 concentrations relative to those at 21% O_2 were 82%, 211%, 148%, and 130% after 0, 1, 2, and 4 d, respectively (Table I).

Dark treatment of pea plants led to a drastic inhibitory effect on nodule activity. After only 1 d of dark, in vivo nitrogenase activity was almost abolished, whereas total root respiration declined by 68% and the ODB resistance was enhanced by 10-fold (Table I). However, there was no effect on the carbon cost of nitrogenase, and Lb and soluble protein only decreased by 29% and 14%, respectively. Prolongation of dark stress for 1 more d lowered Lb content by an additional 63% but had no effect on total soluble pro-

Table I. *Some general markers of metabolic activity in senescing nodules of bean treated with nitrate and of pea treated with darkness for 0, 1, 2, and 4 d*

Means ($n = 4–8$) were compared by one-way analysis of variance and the Duncan's range test. For each parameter and legume species, means denoted by the same letter do not differ significantly at $P < 0.05$.

Parameter	Bean				Pea			
	0 d	1 d	2 d	4 d	0 d	1 d	2 d	4 d
Nitrogenase activity[a] (μmol H_2 min^{-1} $plant^{-1}$)	1.66a	0.45b	0.29b	0.20b	0.76a	0.03b	0.00b	0.00b
Nitrogenase activity in O_2[b]	1.36a	0.95b	0.43c	0.26c	0.56a	0.04b	0.00b	0.00b
Total root respiration (μmol CO_2 min^{-1} $plant^{-1}$)	5.24a	4.76a	5.33a	5.59a	3.23a	1.03b	0.63bc	0.46c
ODB resistance (s $cm^{-1} \times 10^{-6}$)	0.67a	1.98b	1.87b	1.90b	1.47a	15.01b	ND[c]	ND
Carbon cost of nitrogenase (mol CO_2 mol^{-1} H_2)	1.90a	2.10ab	3.30bc	4.56c	2.02a	2.36a	ND	ND
Lb (nmol g^{-1} fresh wt)	221a	260b	205a	102c	121a	86b	32c	22c
Soluble protein (mg g^{-1} fresh wt)	12.4a	16.0b	12.1a	8.6c	14.2a	12.2b	12.2b	12.9ab

[a] Maximum H_2 production under Ar/21% O_2. [b] Maximum H_2 production at increased O_2 concentrations following the Ar-induced decline. [c] ND, Not determined.

Table II. *Carbohydrate content in senescing nodules of bean treated with nitrate and of pea treated with darkness for 0, 1, 2, and 4 d*

Metabolite[a]	Bean				Pea			
	0 d	1 d	2 d	4 d	0 d	1 d	2 d	4 d
	μg g⁻¹ fresh wt							
Glc	173a	104b	92b	51c	348a	109b	125b	94b
Fru	89a	120b	53c	52c	70a	33b	11c	10c
Suc	4445a	3087b	1902c	1111d	8946a	313b	207b	34c
Starch	1095a	652b	466b	521b	8002a	2084b	1526b	1235b

[a] Statistical analysis of means ($n = 3$) was performed as for Table I.

tein. There were no further significant changes after 4 d of darkness, except for total root respiration, which decreased by 86% relative to control (Table I). Increasing rhizosphere O_2 concentrations above 21% caused a slight rise in nitrogenase activity in pea after 1 d of dark, but did not induce any recovery of activity after 2 and 4 d of continuous darkness.

Carbohydrates

Nitrate had considerably less effect on nodule carbohydrates than dark stress. Treatment of bean plants with nitrate led to a progressive decline in Glc, Suc, and starch, whereas Fru increased by 35% after 1 d and declined to 60% of the control value after 2 or 4 d (Table II). The contents of Glc and Suc decreased by 30% to 40% after 1 d of nitrate application, 47% to 57% after 2 d, and 75% after 4 d. Starch was similarly affected after 1 and 2 d with nitrate, but remained at 48% of control after 4 d (Table II).

In contrast, nodules of pea plants dark-treated for 1 d had lost 97% of their Suc content, along with 69% of Glc, 53% of Fru, and 74% of starch (Table II). The contents of Glc and starch remained essentially constant at this low level following prolongation of the dark treatment to 2 or 4 d, whereas Fru declined by 85% relative to control and Suc virtually disappeared after 4 d (Table II).

Antioxidant Enzymes

Nitrate application for 1 d had only a minor effect on antioxidant enzyme activities from bean nodules, with the exception of GR activity, which increased by 41% (Table III). Following 2 d with nitrate, only APX activity had decreased significantly with respect to control, but after 4 d there was a general decline in activities of all enzymes of the ascorbate-GSH cycle. The decreases ranged from approximately 20% for DR and GR to 63% for APX. Catalase activity responded quite differently, with no variation after 2 d of nitrate supply and a 52% decline after 4 d (Table III).

Likewise, after 1 d of dark stress, pea nodules did not show apparent changes in antioxidant activities, but after 2 d there were decreases of 26% to 32% in APX and GR, and catalase activity increased by 31% (Table III). Following 4 d of dark treatment, there were major declines in the activities of the enzymes of the ascorbate-GSH cycle: 40% to 50% for APX, GR, and MR, and 82% for DR. In contrast, catalase activity exceeded the control value by 44% (Table III).

Antioxidant Metabolites and Nucleotides

Some improvements of an HPLC method based on the derivatization of thiols to form highly fluorescent adducts (Fahey and Newton, 1987) allowed us to quantify separately GSH and hGSH in nodules (Table IV). Control (untreated) bean nodules contained 103 nmol GSH and 262 nmol hGSH g^{-1} fresh weight, and pea nodules contained 698 nmol GSH and 90 nmol hGSH g^{-1} fresh weight. Therefore, GSH was the major thiol (89%) in pea nodules, whereas hGSH predominated (72%) in bean nodules. Assuming uniform distribution and 85% water content in nodules, the total thiol tripeptide (GSH + hGSH) concentrations in bean and pea nodules were estimated to be 0.4 and 0.9 mM, respectively.

As occurred with antioxidant enzyme activities, nitrate application for 1 or 2 d had only a very limited effect on the content of antioxidant metabolites and pyridine nucleotides in bean nodules (Table IV). After 1 d with nitrate, there were only minor or moderate changes in GSH (37% decrease), ascorbate (20% increase), and NADH and $NADP^+$ (18% decrease). The contents of other nucleotides

Table III. *Antioxidant enzyme activities in senescing nodules of bean treated with nitrate and of pea treated with darkness for 0, 1, 2, and 4 d*

Enzyme[a]	Bean				Pea			
	0 d	1 d	2 d	4 d	0 d	1 d	2 d	4 d
	μmol min⁻¹ g⁻¹ fresh wt							
APX	8.67a	8.62a	6.17b	3.20c	8.91a	7.49b	6.59b	4.49c
DR	0.67a	0.77b	0.70ab	0.55c	0.17a	0.13ab	0.09b	0.03c
GR	0.41a	0.58b	0.48a	0.33c	0.62a	0.60a	0.42b	0.36b
MR	3.20a	3.30a	2.62ab	1.83b	1.65a	1.52a	1.42a	1.00b
Catalase	1340a	1390a	1340a	640b	160a	160a	210b	230c

[a] Statistical analysis of means ($n = 6–8$) was performed as for Table I.

Table IV. *Antioxidant metabolites and nucleotides in senescing nodules of bean treated with nitrate and of pea treated with darkness for 0, 1, 2, and 4 d*

Metabolite[a]	Bean				Pea			
	0 d	1 d	2 d	4 d	0 d	1 d	2 d	4 d
	nmol g^{-1} fresh wt							
Ascorbate	840a	1010b	950b	840a	460a	340b	300b	210c
GSH[b]	103a	65b	75b	37c	698a	570a	378b	58c
hGSH[b]	262a	224ab	187b	40c	90a	106a	110a	36b
Oxidized thiols[c]	2a	1a	2a	5b	16a	14a	20b	19b
NAD^+	32.3a	29.4ab	26.1b	17.8c	29.2a	18.8b	13.6bc	10.2c
NADH	3.6a	2.9b	2.5bc	2.2c	11.3a	7.1b	4.3bc	3.3c
$NADP^+$	9.3a	7.6b	6.7b	4.1c	4.7a	4.6a	2.9b	2.5b
NADPH	5.0a	4.6a	4.6a	4.9a	4.9a	3.9ab	3.7b	3.3b

[a] Statistical analysis of means (n = 4–12) was performed as for Table I. [b] Determined by the HPLC method. [c] The percentage of thiol tripeptides in the disulfide form was determined by the enzymatic method.

and hGSH remained essentially constant, as did the proportion of the disulfide forms of GSH and hGSH. Following 2 d with nitrate, both GSH and hGSH decreased by 28%, but this decrease was not due to simple thiol oxidation, since 98% of total thiols were still present in the reduced form. Only after 4 d was there a significant but modest increase in the proportion of the disulfide forms from 2% to 5%. At this stage, GSH and hGSH had declined by 64% and 85%, respectively, and pyridine nucleotides, except NADPH, by 39% to 56%. In contrast, the ascorbate content of nodules treated with nitrate for 4 d was identical to that of untreated nodules (Table IV).

The effect of prolonged darkness on pea nodule antioxidants and nucleotides was also moderate after 1 d, with decreases in the range of 26% to 37% for ascorbate, NAD^+, and NADH (Table IV). After 2 d, all parameters except the hGSH content experienced substantial declines ranging from approximately 24% for NADPH to 62% for NADH. In addition, the proportion of oxidized thiols rose significantly, from 14% to 20%. After 4 d, ascorbate and hGSH declined by approximately 60% and GSH by 92%. The nodule content of pyridine nucleotides also decreased markedly, albeit to a lower extent for NAD(H) than for NADP(H). Nevertheless, the NAD^+ to NADH and the $NADP^+$ to NADPH ratios were kept at approximately 3 and 1, respectively, throughout the dark treatment.

Synthesis of GSH and hGSH

Because the nitrate and dark treatments led to major declines of GSH and hGSH in nodules that could not be accounted for by oxidation to the disulfide forms (Table IV), we decided to investigate whether there is GSH and hGSH synthesis in nodules and, if so, whether this can be impaired by the stress treatments. Optimization of previous HPLC methods enabled us to assay all the enzyme activities required for the synthesis of GSH and hGSH in nodules (Table V), indicating that there is genuine synthesis of thiol tripeptides in the nodule tissue. The first committed step for the synthesis of both tripeptides is catalyzed by γECS, and this activity was similar in control (untreated) bean and pea nodules. The second step is thought to be catalyzed by specific synthetases, either GSHS or hGSHS. Both activities were present in bean and pea nodules, but hGSHS activity predominated in bean nodules, whereas GSHS activity predominated in pea. This is in agreement with the major thiol tripeptides found in the respective nodules (Table IV), which strongly suggests that the relative abundance of GSH and hGSH is determined at least in part by the corresponding thiol tripeptide synthetase activities.

Nitrate supply of bean plants for 2 d led to decreases of 40% in γECS activity and 60% in GSHS activity, but had no effect on hGSHS activity; prolongation of treatment up to 4 d led to a decline of 50% to 60% for all three activities of nodules (Table V). Placement of pea plants in the dark for 2 d caused decreases of 40% in GSHS and hGSHS activities of nodules; after 4 d, these activities had decreased by 50% to 60%, whereas the γECS activity of nodules had increased by 55% relative to control (Table V).

Table V. *Activities of enzymes involved in GSH and hGSH synthesis in senescing nodules of bean treated with nitrate and of pea treated with darkness for 0, 2, and 4 d*

Enzyme[a]	Bean			Pea		
	0 d	2 d	4 d	0 d	2 d	4 d
	nmol min^{-1} g^{-1} fresh wt					
γECS	5.5a	3.3b	2.3c	4.9a	5.5a	7.6b
GSHS	1.0a	0.4b	0.4b	18.0a	11.1b	9.3c
hGSHS	9.8a	9.6a	5.0b	12.0a	7.1b	4.5c

[a] Statistical analysis of means (n = 3–4) was performed as for Table I.

Oxidant Damage

The contents of lipid peroxides (malondialdehyde) and oxidatively modified proteins (carbonyl groups) were used as markers of free radical damage in nodules. The response of both parameters during senescence was, however, distinctly different (Table VI). Nitrate treatment of bean or dark treatment of pea for 4 d caused decreases of 39% to 48% in the content of lipid peroxides of nodules. In contrast, both nitrate and prolonged darkness increased the amount of oxidized proteins in nodules by approximately 30% (Table VI).

Immunolocalization of Nitrogenase and APX

Immunogold localization of nitrogenase with silver enhancement and dark-field light microscopy indicated the presence of abundant protein in the infected cells of control (untreated) bean (Fig. 1A) and pea (data not shown) nodules. Little or no labeling occurred in nodules that had been exposed to either of the stress treatments for 4 d (Fig. 1B). Using the same technique but with bright-field light microscopy, APX protein was found to be localized predominantly in the endodermis and adjacent cell layers of the nodule parenchyma (inner cortex), as well as in the infected zone of control bean nodules (Fig. 2A). Using immunofluorescence with the secondary antibody conjugated to the fluorophore Cy3, a similar distribution of APX protein was noticed in control pea nodules (Fig. 2C). Treatment with either nitrate or dark led to a substantial decrease in labeling intensity in both bean and pea nodules (Fig. 2, B and D), in agreement with the observed declines in enzyme activity (Table III). As expected, bean and pea nodule sections in which rabbit normal serum was used in place of the primary antibody showed only very sparse background labeling.

The pattern of immunolocalization of APX at the electron microscopy level was similar to that observed at the light microscopy level. No label was evident in negative controls (Fig. 3, A and B), whereas strong labeling was present in the cytosol of the parenchyma and infected cells of control bean and pea nodules (Fig. 3, C and D). Label was also noted in the cytosol of interstitial cells (Fig. 4B), over the symbiosomes, and occasionally over the mitochondria and bacteroids (Fig. 4C). Immunolabeling of APX decreased in bean and pea nodule tissue with nitrate and dark stress. The location of labeling was not affected by either of the two treatments.

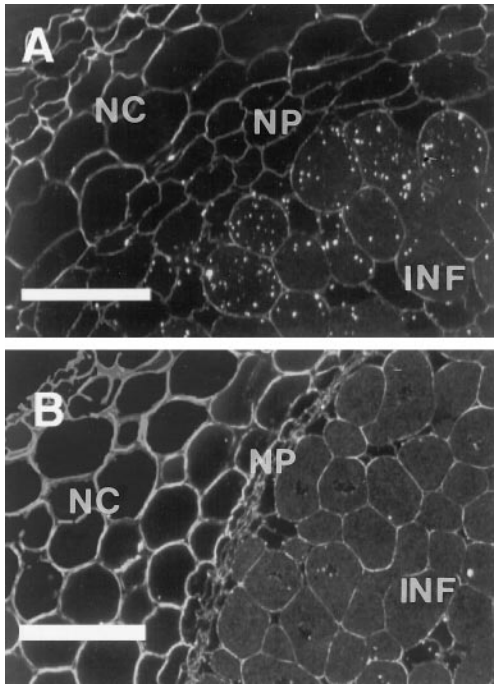

Figure 1. Immunolocalization of nitrogenase in bean nodules using dark-field light microscopy. A, Control (untreated) nodules. Bright spots in the infected zone of this section indicate the presence of nitrogenase. B, Nodule after 4 d with nitrate. Note the almost complete lack of staining in this section. NC, Nodule cortex; NP, nodule parenchyma; INF, infected zone. Bars = 100 μm.

Ultrastructural Studies

Ultrathin sections of representative nodules from nitrate-treated bean and dark-treated pea were also examined by electron microscopy to follow the structural changes occurring during senescence, and complement the physiological and biochemical data. In addition, nodules from dark-treated bean and nitrate-treated pea were processed in parallel to allow for orthogonal comparisons.

Infected cells of control (untreated) bean nodules were densely packed with symbiosomes, each enclosing one to four bacteroids. Bacteroids contained abundant poly-β-hydroxybutyrate granules, and organelles of the infected cell, including mitochondria and plastids, were confined to the periphery of the cell. Bean nodules treated for 1 or 2 d with nitrate essentially had features similar to control nodules (Fig. 4D). After 4 d of nitrate treatment, significant disruption of the host cytoplasm and of symbiosome mem-

Table VI. *Oxidant damage of lipids and proteins in senescing nodules of bean treated with nitrate and of pea treated with darkness for 0, 1, 2, and 4 d*

Parameter[a]	Bean				Pea			
	0 d	1 d	2 d	4 d	0 d	1 d	2 d	4 d
Lipid peroxides	0.27a	0.27a	0.16b	0.14b	1.66a	1.16b	0.88b	1.02b
Oxidized proteins	16.6a	16.4a	18.6a	22.3b	12.8a	15.3ab	17.3b	16.7b

[a] Statistical analysis of means ($n = 4-8$) was performed as for Table I. Lipid peroxides are expressed in nmol malondialdehyde mg^{-1} lipid and oxidized proteins in nmol carbonyl groups mg^{-1} protein.

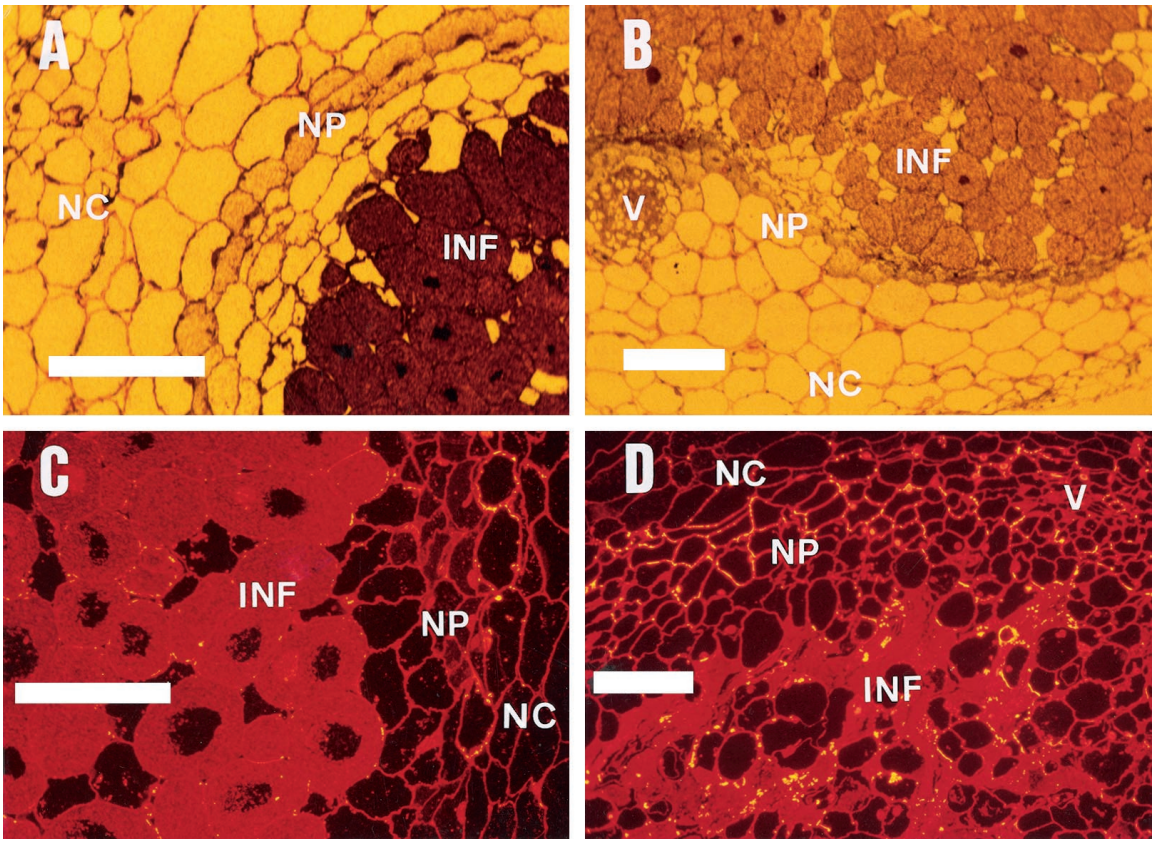

Figure 2. Immunolocalization of APX in nodules of bean (A and B, bright-field immunogold detection) and pea (C and D, immunofluorescent Cy3 detection). A and C, Control (untreated) nodules showing strong labeling in the infected zone and a prominent band in the nodule parenchyma. B, Nodules after 4 d with nitrate. D, Nodules after 4 d of dark stress. B and D show a marked decrease in labeling in both the infected zone and nodule parenchyma. V, Vascular bundle. Other symbols are as in the legend to Figure 2. Bars = 100 μm.

branes was observed; however, there were no evident changes in bacteroids or in poly-β-hydroxybutyrate content (Fig. 4E).

Dark stress resulted in observable changes in bean nodules after only 1 d of treatment (Fig. 4F). Many infected cells, particularly toward the interior of the nodule, showed disrupted cytoplasm and discontinuities in the symbiosome membrane. After 2 d of dark, breaks in the symbiosome membrane were more frequently observed, and cytoplasmic breakdown of infected cells was evident (Fig. 4G). Cell disruption was observed throughout the infected zone of the nodule after 4 d of dark treatment and no intact symbiosomes were evident; however, the integrity of bacteroids was not affected and poly-β-hydroxybutyrate granules were comparable in appearance to those observed in controls (Fig. 4H).

Control pea nodules contained abundant symbiosomes within the dense host cytoplasm. No poly-β-hydroxybutyrate was observed within the bacteroids (Fig. 5, A–C). Cell organelles were located at the periphery of infected cells, and profiles of the rough ER and Golgi apparatus were often apparent. One day of dark resulted in minimal changes in infected cells (Fig. 5C). Following 2 d of dark treatment, cytoplasmic disruption was widespread, including cytoplasmic breakdown and lesions in the symbiosome membranes (Fig. 5D). Bacteroids ranged in appearance from those showing slight cytoplasmic disruption to others showing extensive breakdown. After 4 d of dark, bacteroids were often misshapen, with disrupted cytosplasm and symbiosome membranes (Fig. 5E). The host cell cytoplasm was not discernible and host cell organelles were rarely observed.

One day of nitrate treatment had little effect on the appearance of infected cells in pea nodules. Cell plasmolysis and discontinuities in the symbiosome membrane were apparent after 2 d with nitrate (Fig. 5F). Bacteroids with irregular membranes were occasionally observed (Fig. 5G). Cytoplasmic and bacteroid degeneration was extensive following 4 d of nitrate treatment, and cellular detail was difficult to discern (Fig. 5H).

Ferritin Localization

Preliminary immunoblots of ferritin showed that the antibody raised to soybean seed ferritin recognized a single protein band of 28 kD, characteristic of ferritin subunits, in bean nodule extracts. As expected, a positive control consisting of a soluble extract of tobacco leaves overexpressing soybean ferritin produced an identical band (Fig. 6). The

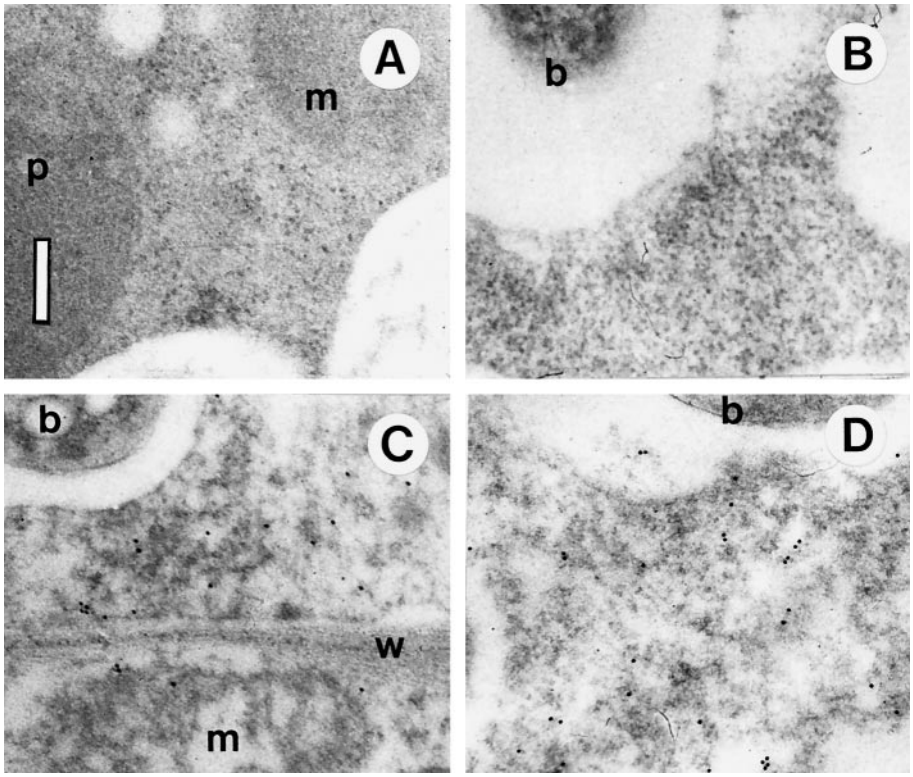

Figure 3. Immunogold localization of APX in control (untreated) nodules. A and B, Negative controls (normal rabbit antiserum in place of APX antibody) of bean and pea nodules, respectively, showing no label in the cytosol or organelles of infected cells. C and D, Bean and pea nodule sections, respectively, showing APX label over the cytosol of infected cells. b, Bacteroid; w, cell wall; m, mitochondrion; p, plastid. The bar in A = 0.2 μm for all panels.

immunoblots also revealed that ferritin accumulated in bean nodules in response to nitrate treatment (Fig. 6).

The soybean antibody, however, exhibited very poor reactivity with pea ferritin (data not shown). Consequently, ferritin was only immunolocalized in bean nodules. Control (untreated) bean nodule sections showed little labeling for ferritin (Fig. 7A), but this was clearly visible after 2 or 4 d of nitrate treatment (Fig. 7, B–D), confirming blot analysis. After 2 d with nitrate, ferritin was localized in the plastids and amyloplasts of uninfected and infected cells, and occasionally over the bacteroids. The heaviest labeling was observed in the amyloplasts of the uninfected interstitial cells and of the parenchyma cells (Fig. 7, B and C). In some sections, scattered arrays or small clusters of ferritin particles could be seen in the amyloplasts without the assistance of gold labeling (Fig. 7B). After 2 d (and especially after 4 d) of nitrate treatment, large ferritin aggregates were easily observed in the amyloplasts (Fig. 7, C and D). Quite often, these large deposits did not show any immunolabeling, although it was observed in plastids or amyloplasts within the same nodule sections (Fig. 7C), indicating that the antibody was recognizing isolated ferritin particles and smaller ferritin deposits.

DISCUSSION

In this work we have obtained simultaneously an array of physiological, biochemical, and structural data for bean and pea nodules induced to senesce by treating the plants with nitrate or prolonged darkness. This allowed us to monitor the progress of nodule senescence in a controlled manner and to discern more readily between the reversible and irreversible stages of stress application.

Nitrate-Induced Legume Nodule Senescence

Nitrate had a two-stage effect on bean nodules. In the first stage (1–2 d), there were major declines in the in vivo nitrogenase activity and increases in the ODB resistance and carbon cost of nitrogenase, but only moderate or no changes in the nodule content of carbohydrates, antioxidants, and pyridine nucleotides; furthermore, there were significant increases in Lb, soluble protein, and ascorbate. At this early stage, there were no detectable changes in the nodules at the ultrastructural level. Therefore, it would appear that the decrease of nitrogenase activity after 1 to 2 d may be attributed to O_2 limitation at the ODB level and not to biochemical factors such as degradation of nitrogenase or Lb, oxidative damage of cell components, or sugar deprivation of host cells or bacteroids. However, the causal relationship between nitrogenase activity and ODB operation cannot be fully examined by the present data, and it is possible that nitrogenase activity is decreased by an as yet unknown mechanism that results in closure of the ODB.

O_2 limitation through the ODB was confirmed by the partial recovery of nitrogenase activity in nitrate-treated

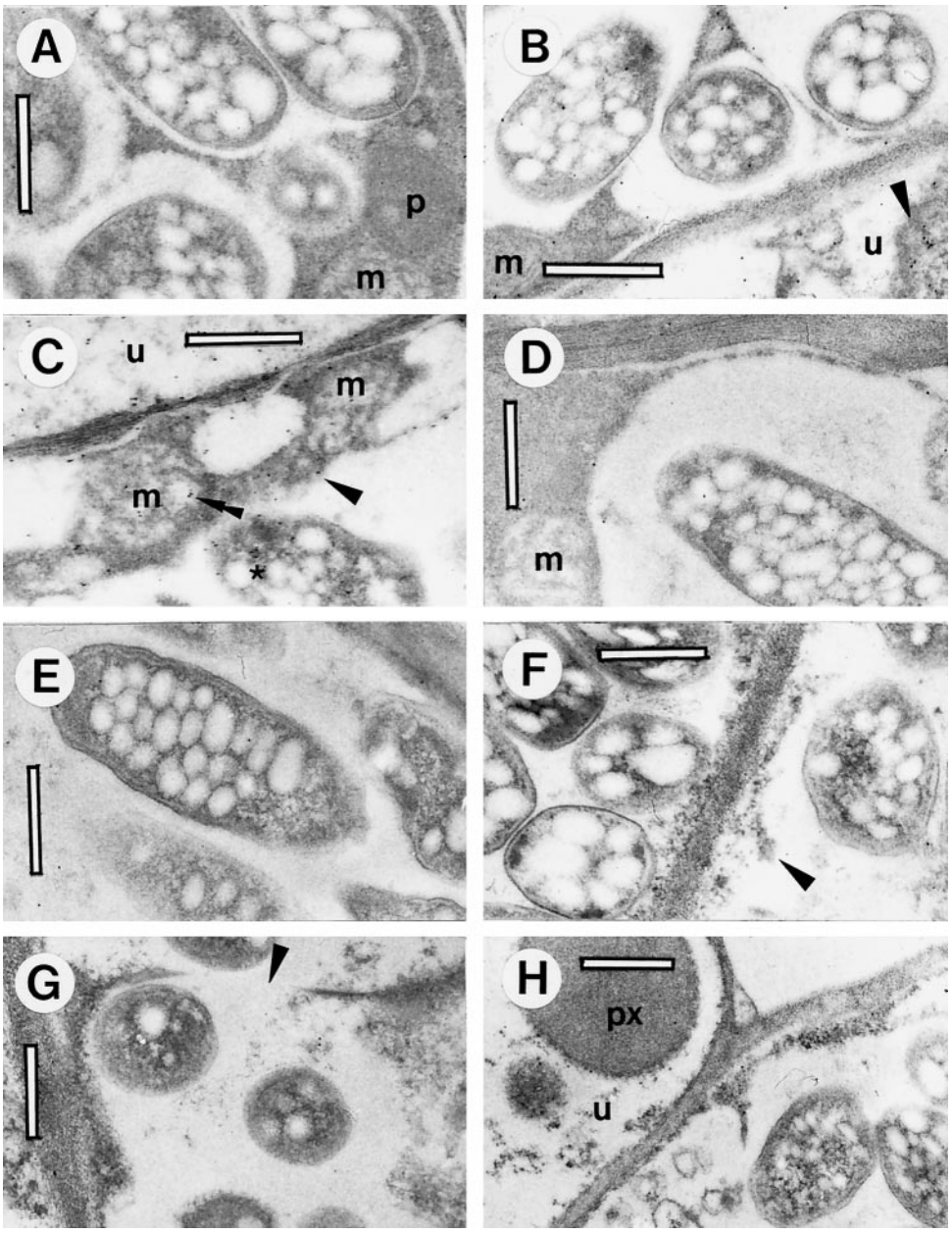

Figure 4. Ultrastructural changes and APX localization in bean nodules after nitrate and dark treatments. A, Negative control showing no label in the cytosol, organelles, or symbiosome of a control (untreated) nodule. B and C, Control nodules showing APX localization in uninfected and infected cells. Label is seen frequently in the cytosol of both uninfected (B, arrowhead) and infected (C, arrowhead) cells, over the symbiosome, and occasionally over mitochondria (C, double arrowhead) and bacteroids (C, asterisk). D, Detail of infected cell of the nodule after 2 d of nitrate treatment. Cells and bacteroids are similar in appearance to controls. E, Detail of infected cell of the nodule after 4 d with nitrate showing the absence of symbiosome membrane, but little change in bacteroids or in poly-β-hydroxybutyrate granules. F, Detail of infected cells of the nodule after 1 d of dark stress showing disruption of the cytoplasm (arrowhead). Symbiosome membranes are disrupted in both of the cells shown. G, Infected cells of nodule after 2 d of dark stress showing lesions in the symbiosome membrane and the cytoplasmic disruption observed throughout the nodule. H, Nodule following 4 d of dark stress showing general disruption of infected and uninfected cells. However, most bacteroids remain intact. m, Mitochondrion; p, plastid; px, peroxisome; and u, uninfected cell. Bars = 0.4 μm.

plants upon increasing the concentration of rhizospheric O_2. This recovery, and the absence of structural and biochemical damage, indicate that at this early stage the effect of nitrate was still reversible. In contrast, in the second stage (4 d), there was an almost complete loss of both nitrogenase activity and protein, along with a marked decline in Lb, soluble protein, sugars, antioxidants (except ascorbate), and nucleotides. There was also a general de-

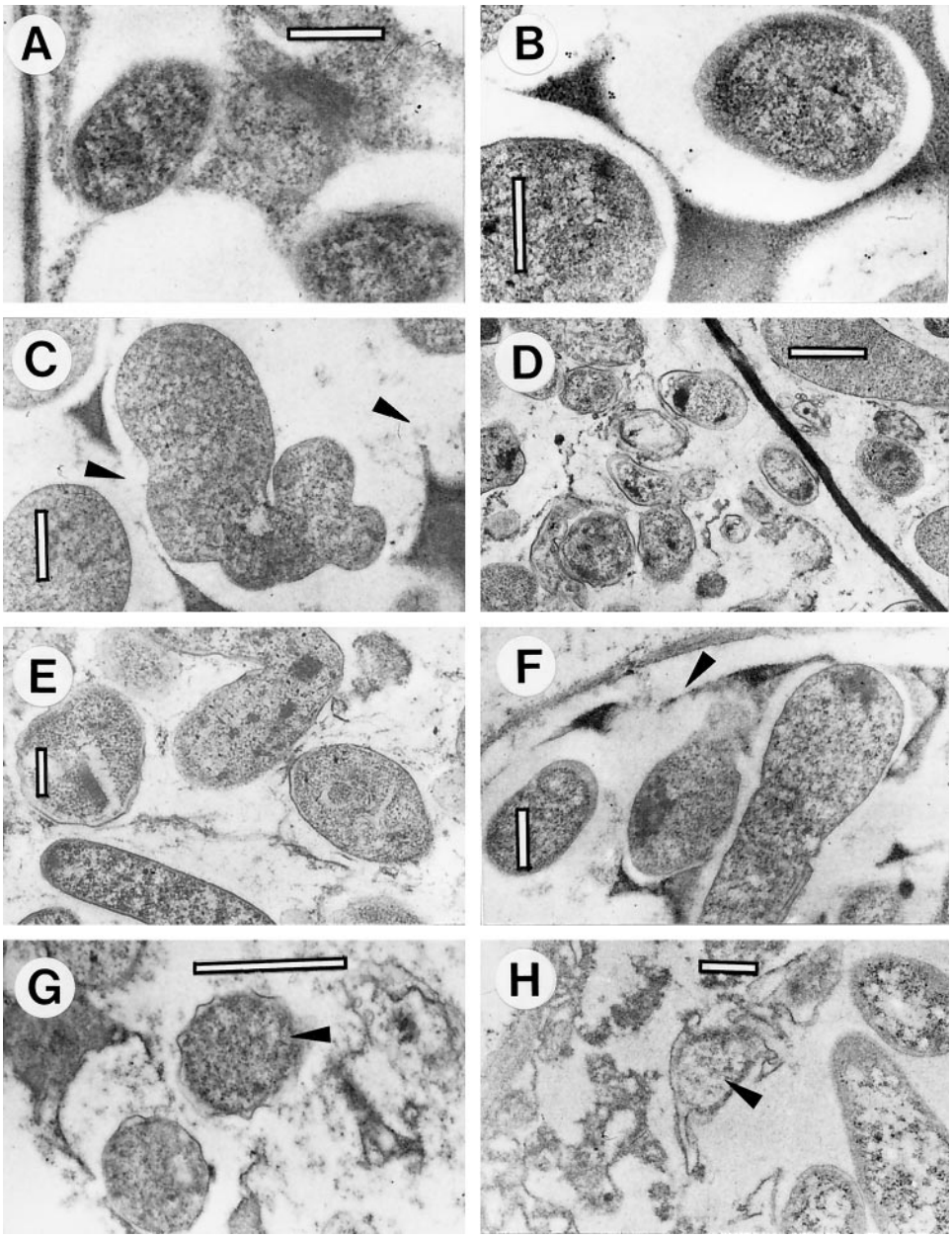

Figure 5. Ultrastructural changes and APX localization in pea nodules after nitrate and dark treatments. A, Negative control showing no label in the cytosol, wall, or symbiosome of an untreated nodule. B, Infected cell of untreated nodule showing distribution of APX label over the cytosol and symbiosome. Label was also observed in uninfected cells and occasionally over mitochondria. C, Infected cell of nodule after 1 d of dark stress showing only minor disruption of symbiosome membrane (arrowhead). D, Low-magnification micrograph of cell after 2 d of dark stress showing the extent of cytoplasmic disruption and bacteroids with various degrees of breakdown. E, Infected cell of the nodule after 4 d of dark stress showing disruption of symbiosome membranes and misshapen, disrupted bacteroids. F and G, Infected cells of nodules after 2 d with nitrate showing some cell plasmolysis (F, arrowhead), discontinuity in the symbiosome membrane, and misshapen bacteroids (G, arrowhead). H, Infected cell of the nodule after 4 d with nitrate showing the extensive cytoplasmic and bacteroid degeneration characteristic of this stage. A, B, C, E, F, and H, Bars = 0.4 μm. D and G, Bars = 2 μm.

terioration of the nodule ultrastructure, in particular of symbiosome membranes, and an accumulation of oxidized proteins. This stage of nitrate inhibition would therefore appear to be essentially irreversible. However, these conclusions await final verification through recovery experiments.

The effects of nitrate on bean and pea nodules can be compared with the limited information available for other legumes. In lupine and clusterbean nodules, nitrogenase activity (assayed in both cases with a closed system) was inhibited by 35% after 3 to 5 d with 20 mM nitrate, and structural degradation of lupine nodules was only recognizable after 10 d (Lorenzo et al., 1990; Swaraj et al., 1993). In bean and pea nodules, nitrogenase activity (assayed in both cases with a flow-through gas system) was inhibited

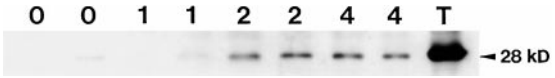

Figure 6. Western analysis of ferritin in bean nodules using chemiluminiscence detection. Lanes 0, 1, 2, and 4 were loaded with soluble extracts (20 μg protein) from nodules treated with nitrate for 0, 1, 2 and 4 d. Two extracts obtained independently were loaded for each treatment. Lane T was loaded with a soluble extract (20 μg protein) of transgenic tobacco leaves overexpressing soybean ferritin (Van Wuytswinkel et al., 1998), which served as a positive control. In all lanes a single band at 28 kD, characteristic of ferritin subunits, was observed.

by approximately 85% after only 2 d with 10 mM nitrate. Structural data revealed differences in the progression of senescence between pea and bean nodules. In pea nodules the plasmolysis of host cells and the disruption of symbiosome membranes and bacteroids were already evident after 2 d, while in bean nodules, nitrate had little effect on the shape or poly-β-hydroxybutyrate content of bacteroids even after 4 d. These data suggest that pea nodules are particularly sensitive to nitrate.

Dark-Induced Legume Nodule Senescence

Prolonged darkness severely affected pea nodule metabolism. After only 1 d of dark there were major effects on total root respiration, ODB resistance, and carbon costs of nitrogenase. In addition there were moderate decreases in Lb and in some antioxidants and nucleotides; however, the most affected parameters were by far the in vivo nitrogenase activity and the nodule Suc content, which decreased by 97%. The almost complete depletion of Suc, the major carbon and energy source for host cell metabolism, along with the substantial decreases in other carbohydrates, is the most likely cause for the limitation of nitrogenase activity in dark-treated pea. This conclusion is supported by immunoblots of nitrogenase showing no loss in the protein after 1 d of dark in both bean (Gogorcena et al., 1997) and pea (data not shown), and is also consistent with the finding that isolated bacteroids from dark-treated soybean retained 50% of the initial nitrogenase activity (Sarath et al., 1986) and fully recovered upon addition of succinate (Carroll et al., 1987). After 2 d of dark, pea nodules showed drastic decreases in Lb and carbohydrates, moderate decreases of many antioxidants, accumulation of modified proteins, and evident symptoms of structural deterioration. After 4 d of dark, there was a general collapse of metabolism and extensive structural damage.

There are some significant differences in the response of other legume nodules to dark stress. Thus, inhibition of nitrogenase activity was much less dramatic in soybean (Sarath et al., 1986) and clusterbean (Swaraj et al., 1994) than it was in bean (Gogorcena et al., 1997) and pea (this work). Also, 2 d of dark had no significant effect on Lb or total soluble protein in nodules of soybean (Pfeiffer et al., 1983; Gordon et al., 1993), clusterbean (Swaraj et al., 1994), or bean (Gogorcena et al., 1997). However, in pea nodules, the same treatment caused a 74% decline in Lb but only a 14% decline in total soluble protein, which is indicative of a relatively high sensitivity of pea Lb to degradation com-

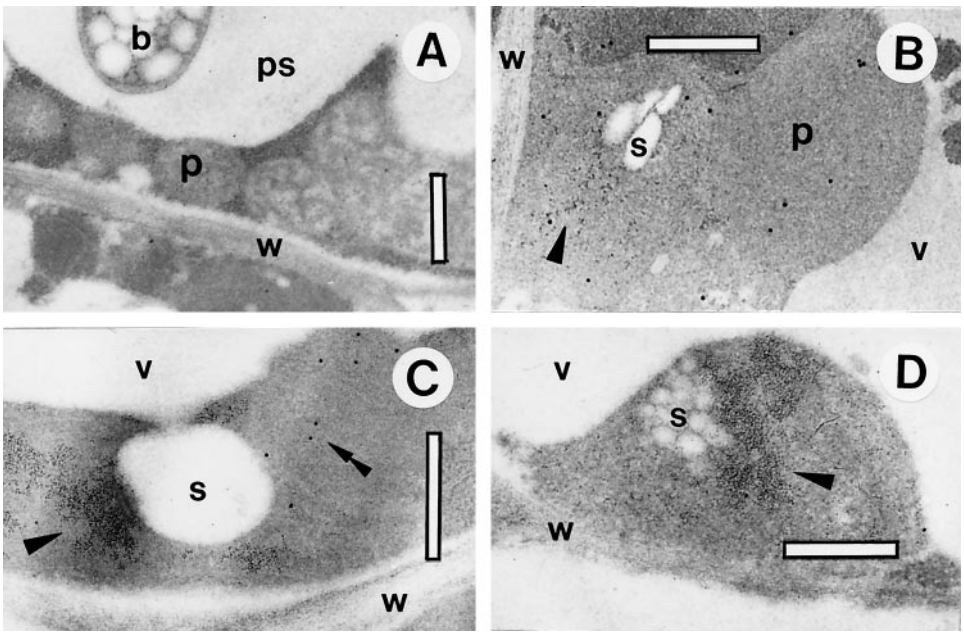

Figure 7. Electron micrographs of bean nodules showing ferritin localization. A, Control (untreated) nodule section showing scant deposition of gold label over infected and uninfected cells. B, Detail of parenchyma cell after 2 d with nitrate showing ferritin localization in plastids and amyloplasts. A linear array of ferritin particles (arrowhead) is visible in the amyloplast. C, Detail of parenchyma cell after 2 d with nitrate showing large ferritin deposits not labeled with gold (arrowhead) as well as disperse labeling of ferritin particles (double arrowhead) in the amyloplast. D, Amyloplast from a parenchyma cell after 4 d with nitrate. A large aggregate of ferritin (arrowhead) is present, but did not label with gold. b, Bacteroid; p, plastid; ps, peribacteroid space; s, starch grain; v, vacuole; w, cell wall. Bars = 0.4 μm.

pared with other cytosolic proteins. This conclusion is consistent with an early observation that exposure of pea plants to 3 d of dark was sufficient to induce greening of nodules and breakdown of 50% of total heme (Roponen, 1970). Because the pathway for Lb degradation in vivo is largely unknown, it can only be speculated that the rapid loss of pea Lb in dark-stressed nodules is due to a particularly rapid activation or decompartmentation of proteases located in the infected cells that display a high affinity for Lb, especially at the acidic intracellular pH of senescing nodules (Pladys et al., 1991).

Thiols, APX, and Ferritin in Senescent Legume Nodules

Three important antioxidants, GSH and APX, which are critical for the operation of the ascorbate-GSH cycle, and ferritin, which is critical for the control of the cellular concentration of catalytic iron, have been studied in further detail to extend earlier studies on the mechanism of stress-induced nodule senescence.

An enzymatic method (Griffith, 1980) was previously employed to estimate the concentration of GSH in nodules. Because this method could not distinguish between GSH and hGSH (Klapheck, 1988), and because it was uncertain whether hGSH was present in nodules, we estimated the concentration of total tripeptides in pea and bean nodules as 0.9 mM (Escuredo et al., 1996; Gogorcena et al., 1997). Using HPLC, we found in this work that hGSH is present in nodules at variable concentrations: 0.12 mM GSH and 0.31 mM hGSH for bean nodules, and 0.82 mM GSH and 0.11 mM hGSH for pea nodules. Thus, the enzymatic method tends to overestimate the thiol content in plant tissues having primarily hGSH, because the reaction of yeast GR with hGSH is faster than with GSH (Klapheck, 1988). For pea nodules, which mainly contain GSH, both methods yielded similar results.

An obvious question raised in this work is why hGSH is the major thiol in bean nodules. Although this cannot be answered at present, our results show that the relative abundance of GSH and hGSH in nodules is likely to be dictated by the presence of specific tripeptide synthetases: hGSHS in bean nodules and GSHS in pea nodules. This conclusion is reinforced by the partial purification of distinct enzymes from pea (GSHS) and mungbean (hGSHS) leaves (Macnicol, 1987), which contain only GSH and hGSH, respectively (Klapheck, 1988). The fact that hGSH is the only thiol tripeptide present in the leaves of some legumes also implies that the corresponding chloroplasts have a functional ascorbate-hGSH pathway to avoid photooxidative damage, and that hGSH and GSH share at least some antioxidative role in vivo.

The drastic decreases of the major thiols after 4 d of treatment (85% hGSH in bean nodules and 92% GSH in pea nodules) cannot be accounted for by oxidation to the disulfide forms or by the 50% to 60% decline in GSHS and hGSHS activities. Nor can it be ascribed to a limitation of γECS activity, either directly (the activity only declined by 60% in bean nodules and increased moderately in pea nodules) or through the availability of Cys (the content of this substrate decreased by 50%–60% in both bean and pea nodules after 4 d of treatment). The lack of evidence for a marked inhibition of thiol synthesis, together with the extensive Lb degradation and oxidative reactions taking place in stressed nodules that are manifest by a loss of Lb heme and accumulation of oxidized proteins, may provide a clue for the large decline in GSH and hGSH. These thiols may be consumed by nonenzymatic reactions with activated oxygen species or by enzymatic degradation, with the possible formation of mixed disulfides between thiols and proteins (Rennenberg, 1995). These aspects of thiol catabolism in nodules, and in plants in general, remain virtually unexplored.

Another antioxidant, APX, is critical for the disposal of H_2O_2 in nodules. The APX protein was predominantly located to the parenchyma and infected zone, confirming a previous report in which APX protein and mRNA were shown to be enhanced in the parenchyma and infected cells of alfalfa nodules (Dalton et al., 1998). In the same study, APX protein was also found to be increased in the nodule parenchyma and infected zone of several determinate nodules (Dalton et al., 1998). Our electron microscopy studies corroborate the heterogeneous distribution of APX within nodules and indicate that the protein is very abundant in the cytosol of infected cells. The observation of occasional labeling of APX in the mitochondria would explain the detection of enzyme activity in purified mitochondria from soybean nodules (Dalton et al., 1993). The activity and content of APX protein largely decreased in senescent nodules, which may cause a lowering in protection against H_2O_2 generated by the respiratory activity of the nodule parenchyma and infected cells.

Finally, we conducted studies to localize ferritin in bean nodules and to determine the changes in ferritin content during senescence. Ferritin was barely detectable in control nodules but accumulated in nodules treated with nitrate for 2 or 4 d. The very low content of ferritin protein found in mature, untreated bean nodules is in agreement with the observation that ferritin accumulates in young soybean nodules but declines in mature nodules, when iron storage is apparently no longer required (Bergersen, 1963; Ragland and Theil, 1993). Ferritin was predominantly found in the plastids and amyloplasts of interstitial cells in the infected zone and in the parenchyma cells. The subcellular location of ferritin in bean nodules is fully consistent with other reports showing ferritin particles in plastids and amyloplasts of soybean, alfalfa, and lupine nodules (Bergersen, 1963; Lucas et al., 1998), in amyloplasts of soybean cell cultures (Briat and Lobréaux, 1997), and in chloroplasts and other plastids of several plants (Seckback, 1982).

The scattered arrays and large deposits of ferritin particles observed after 2 or 4 d with nitrate closely resemble, respectively, the F-2 and F-3 types described by Seckback (1982). The latter category is defined as paracrystalline ferritin arrangements (sometimes including small zones of crystalline structure), such as those observed in plastids of iron-treated *Xanthium* without the assistance of gold labeling. Our finding that the paracrystalline deposits of ferritin-like material did not label as densely as would be expected with the soybean antibody requires further investigation, but similar ferritin structures, clearly immunola-

beled, accumulate in the cortex of senescing soybean and lupine nodules (Lucas et al., 1998).

Ferritin synthesis in plants is regulated by iron and is induced by various adverse conditions, including iron overload, which lead to oxidative stress (Briat and Lobréaux, 1997). Recent experiments with de-rooted maize plantlets have shown that H_2O_2 induces ferritin mRNA accumulation in the presence of low iron concentrations and that this effect is prevented by pretreatment of plantlets with antioxidants, indicating that the induction of ferritin gene expression in this system requires an oxidative step (Briat and Lobréaux, 1997). Based on these observations, our results showing ferritin protein accumulation in senescent bean nodules may be interpreted as a response to oxidative stress. This oxidative stress is evidenced by the accumulation of damaged proteins in nitrate-treated bean nodules and is probably a consequence of the lowering of antioxidant activities and the release of catalytic iron from proteins (Becana et al., 1998). Further work is needed to establish the mechanism for ferritin induction in nitrate-treated bean nodules and to determine whether a similar phenomenon occurs in other legume nodules under different types of stress.

ACKNOWLEDGMENTS

We thank Shannon Joyner (Reed College), Caron James (Institute of Grassland and Environmental Research), and Gloria Rodríguez (Estación Experimental de Aula Dei) for technical assistance. We are considerably indebted to Tomas Ruiz-Argüeso (Universidad Politécnica de Madrid) for the Southern analysis of *hup* genes in the two *Rhizobium* strains used in this study, to Paul Ludden (University of Wisconsin, Madison) for providing nitrogenase antibody, to Elizabeth Theil (Children's Hospital Oakland Research Institute, Oakland, CA) and Jean-François Briat (Université de Montpellier II, France) for providing ferritin antibodies and help with western analysis, and to Chris Davitt and Valerie Lynch-Holm (Washington State University, Pullman) for sectioning and embedding samples for light microscopy.

Received April 16, 1999; accepted June 2, 1999.

LITERATURE CITED

Aebi H (1984) Catalase *in vitro.* Methods Enzymol **105:** 121–126

Asada K (1984) Chloroplasts: formation of active oxygen and its scavenging. Methods Enzymol **105:** 422–429

Becana M, Moran JF, Iturbe-Ormaetxe I (1998) Iron-dependent oxygen free radical generation in plants subjected to environmental stress: toxicity and antioxidant protection. Plant Soil **201:** 137–147

Bergersen FJ (1963) Iron in the developing soybean nodule. Aust J Biol Sci **16:** 916–919

Bligh EG, Dyer WJ (1959) A rapid method of total lipid extraction and purification. Can J Biochem Physiol **37:** 911–917

Briat JF, Lobréaux S (1997) Iron transport and storage in plants. Trends Plant Sci **2:** 187–193

Carroll BJ, Hansen AP, McNeil DL, Gresshoff PM (1987) Effect of oxygen supply on nitrogenase activity of nitrate- and dark-stressed soybean (*Glycine max* [L.] Merr.) plants. Aust J Plant Physiol **14:** 679–687

Cohen HP, Sarath G, Lee K, Wagner FW (1986) Soybean root nodule ultrastructure during dark-induced stress and recovery. Protoplasma **132:** 69–75

Cresswell A, Gordon AJ, Mytton LR (1992) The physiology and biochemistry of cultivar-strain interactions in the white clover-*Rhizobium* symbiosis. Plant Soil **139:** 47–57

Dalton DA, Baird LM, Langeberg L, Taugher CY, Anyan WR, Vance CP, Sarath G (1993) Subcellular localization of oxygen defense enzymes in soybean (*Glycine max* [L.] Merr.) root nodules. Plant Physiol **102:** 481–489

Dalton DA, Joyner SL, Becana M, Iturbe-Ormaetxe I, Chatfield JM (1998) Enhanced antioxidant defenses in the peripheral cell layers of legume root nodules. Plant Physiol **116:** 37–43

Dalton DA, Langeberg L, Robbins M (1992) Purification and characterization of monodehydroascorbate reductase from soybean root nodules. Arch Biochem Biophys **292:** 281–286

Dalton DA, Russell SA, Hanus FJ, Pascoe GA, Evans HJ (1986) Enzymatic reactions of ascorbate and glutathione that prevent peroxide damage in soybean root nodules. Proc Natl Acad Sci USA **83:** 3811–3815

Escuredo PR, Minchin FR, Gogorcena Y, Iturbe-Ormaetxe I, Klucas RV, Becana M (1996) Involvement of activated oxygen in nitrate-induced senescence of pea root nodules. Plant Physiol **110:** 1187–1195

Fahey RC, Newton GL (1987) Determination of low-molecular-weight thiols using monobromobimane fluorescent labeling and high-performance liquid chromatography. Methods Enzymol **143:** 85–96

Gogorcena Y, Gordon AJ, Escuredo PR, Minchin FR, Witty JF, Moran JF, Becana M (1997) N_2 fixation, carbon metabolism, and oxidative damage in nodules of dark-stressed common bean plants. Plant Physiol **113:** 1193–1201

González EM, Gordon AJ, James CL, Arrese-Igor C (1995) The role of sucrose synthase in the response of soybean nodules to drought. J Exp Bot **46:** 1515–1523

Gordon AJ, Minchin FR, Skøt L, James CL (1997) Stress-induced declines in soybean N_2 fixation are related to nodule sucrose synthase activity. Plant Physiol **114:** 937–946

Gordon AJ, Ougham HJ, James CL (1993) Changes in levels of gene transcripts and their corresponding proteins in nodules of soybean plants subjected to dark-induced stress. J Exp Bot **44:** 1453–1460

Griffith OW (1980) Determination of glutathione and glutathione disulfide using glutathione reductase and 2-vinylpyridine. Anal Biochem **106:** 207–212

Hell R, Bergmann L (1988) Glutathione synthetase in tobacco suspension cultures: catalytic properties and localization. Physiol Plant **72:** 70–76

Iturbe-Ormaetxe I, Escuredo PR, Arrese-Igor C, Becana M (1998) Oxidative damage in pea plants exposed to water deficit or paraquat. Plant Physiol **116:** 173–181

Klapheck S (1988) Homoglutathione: isolation, quantification and occurrence in legumes. Physiol Plant **74:** 727–732

Klapheck S, Zopes H, Levels HG, Bergmann L (1988) Properties and localization of the homoglutathione synthetase from *Phaseolus coccineus* leaves. Physiol Plant **74:** 733–739

Kocsy G, Brunner M, Rüegsegger A, Stamp P, Brunold C (1996) Glutathione synthesis in maize genotypes with different sensitivities to chilling. Planta **198:** 365–370

LaRue TA, Child JJ (1979) Sensitive fluorometric assay for leghemoglobin. Anal Biochem **92:** 11–15

Law MY, Charles SA, Halliwell B (1983) Glutathione and ascorbic acid in spinach *(Spinacia oleracea)* chloroplasts. Biochem J **210:** 899–903

Layzell DB, Hunt S, Palmer GR (1990) Mechanisms of nitrogenase inhibition in soybean nodules: pulse-modulated spectroscopy indicates that nitrogenase activity is limited by O_2. Plant Physiol **92:** 1101–1107

Levine RL, Garland D, Oliver CN, Amici A, Climent I, Lenz A, Ahn B, Shaltiel S, Stadtman ER (1990) Determination of carbonyl content in oxidatively modified proteins. Methods Enzymol **186:** 464–478

Leyva A, Palacios JM, Murillo J, Ruiz-Argüeso T (1990) Genetic organization of the hydrogen uptake *(hup)* cluster of *Rhizobium leguminosarum.* J Bacteriol **172:** 1647–1655

Lorenzo C, Lucas MM, Vivo A, de Felipe MR (1990) Effect of nitrate on peroxisome ultrastructure and catalase activity in nodules of *Lupinus albus* L. cv. Multolupa. J Exp Bot **41:** 1573–1578

Lucas MM, Van de Sype G, Hérouart D, Hernández MJ, Puppo A, de Felipe MR (1998) Immunolocalization of ferritin in determinate and indeterminate legume root nodules. Protoplasma **204:** 61–70

Macnicol PK (1987) Homoglutathione and glutathione synthetases of legume seedlings: partial purification and substrate specificity. Plant Sci **53:** 229–235

MacRae JC (1971) Quantitative measurement of starch in very small amounts of leaf tissue. Planta **96:** 101–108

Matsumura H, Miyachi S (1980) Cycling assay for nicotinamide adenine dinucleotides. Methods Enzymol **69:** 465–470

May MJ, Vernoux T, Leaver C, Van Montagu M, Inzé D (1998) Glutathione homeostasis in plants: implications for environmental sensing and plant development. J Exp Bot **49:** 649–667

Minchin FR, Witty JF, Sheehy JE, Muller M (1983) A major error in the acetylene reduction assay: decreases in nodular nitrogenase activity under assay conditions. J Exp Bot **34:** 641–649

Minotti G, Aust SD (1987) The requirement for iron (III) in the initiation of lipid peroxidation by iron (II) and hydrogen peroxide. J Biol Chem **262:** 1098–1104

Nakano Y, Asada K (1981) Hydrogen peroxide is scavenged by ascorbate-specific peroxidase in spinach chloroplasts. Plant Cell Physiol **22:** 867–880

Pfeiffer NE, Malik NSA, Wagner FW (1983) Reversible dark-induced senescence of soybean root nodules. Plant Physiol **71:** 393–399

Pladys D, Dimitrijevic L, Rigaud J (1991) Localization of a protease in protoplast preparations in infected cells of French bean nodules. Plant Physiol **97:** 1174–1180

Ragland M, Theil EC (1993) Ferritin (mRNA, protein) and iron concentrations during soybean nodule development. Plant Mol Biol **21:** 555–560

Rennenberg H (1995) Processes involved in glutathione metabolism. *In* RM Wallsgrove, ed, Amino Acids and Their Derivatives in Higher Plants. Cambridge University Press, Cambridge, UK, pp 155–171

Roponen I (1970) The effect of darkness on the leghemoglobin content and amino acid levels in the root nodules of pea plants. Physiol Plant **23:** 452–460

Sarath G, Pfeiffer NE, Sodhi CS, Wagner FW (1986) Bacteroids are stable during dark-induced senescence of soybean root nodules. Plant Physiol **82:** 346–350

Seckback J (1982) Ferreting out the secrets of plant ferritin: a review. J Plant Nutr **5:** 369–394

Sprent JI (1980) Root nodule anatomy, type of export product and evolutionary origin in some Leguminosae. Plant Cell Environ **3:** 35–43

Swaraj K, Laura JS, Bishnoi NR (1993) Nitrate induced nodule senescence and changes in activities of enzymes scavenging H_2O_2 in clusterbean (*Cyamopsis tetragonaloba* Taub.). J Plant Physiol **141:** 202–205

Swaraj K, Laura JS, Bishnoi NR (1994) Dark treatment effects on nitrogen fixation and enzymes associated with scavenging hydrogen peroxide in clusterbean nodules. Plant Physiol Biochem **32:** 115–119

Vance CP, Heichel GH, Barnes DK, Bryan JW, Johnson LE (1979) Nitrogen fixation, nodule development, and vegetative regrowth of alfalfa (*Medicago sativa* L.) following harvest. Plant Physiol **64:** 1–8

Van Wuytswinkel O, Vansuyt G, Grignon N, Fourcroy P, Briat JF (1998) Iron homeostasis alteration in transgenic tobacco overexpressing ferritin. Plant J **17:** 93–97

Witty JF, Minchin FR (1998) Methods for the continuous measurement of O_2 consumption and H_2 production by nodulated legume root systems. J Exp Bot **49:** 1041–1047

Witty JF, Minchin FR, Skøt L, Sheehy JE (1986) Nitrogen fixation and oxygen in legume root nodules. Oxf Surv Plant Mol Cell Biol **3:** 275–314